Title

Methods to Enhance Laser Speckle Imaging of High-Flow and Low-Flow Vasculature

Authors

Choi, Bernard

Ringold, Tyson L

Kim, Jeehyun

Publication Date

2009

DOI

10.1109/iembs.2009.5333204

Published in final edited form as:
Conf Proc IEEE Eng Med Biol Soc. 2009 ; 2009: 4073–4076. doi:10.1109/IEMBS.2009.5333204.

Methods to Enhance Laser Speckle Imaging of High-Flow and Low-Flow Vasculature

Bernard Choi,
Departments of Biomedical Engineering and Surgery, Beckman Laser Institute, University of California, Irvine, CA 92612 USA (choib@uci.edu).

Tyson L. Ringold, and
Department of Mechanical Engineering, University of California, Los Angeles, CA USA. He now is with the School of Mechanical Engineering, Purdue University, West Lafayette, IN 47907 USA (tringold@gmail.com).

Jeehyun Kim
Beckman Laser Institute, University of California, Irvine, CA 92612 USA. He now is with Kyungpook National University, Daegu, Korea (jeehk@knu.ac.kr).

Abstract

The objective of this paper is to present two methods to extend the response range of laser speckle imaging (LSI). We report on the use of two methods (image exposure time control and magnetomotive actuation of exogenous contrast agents) to enhance characterization of high- and low-flow vasculature, respectively. With an exposure time of 10 and 0.01 ms, the linear response range extended to 10 and 280 mm/s, respectively. With application of an AC magnetic field to a solution of stagnant SPIO particles, an apparent increase of ~3× in speckle flow index was induced.

I. Introduction

Laser speckle imaging (LSI) is a simple, noncontact method, used primarily in small-animal imaging studies to characterize blood flow dynamics associated with the microvasculature [1-11]. Experimental comparisons of LSI with laser Doppler flowmetry (LDF) have demonstrated equivalency of the two methods [1, 7, 9]. Similar to LDF, LSI data are typically reported as percent change from baseline, and hence rely on the assumption that a linear response range exists between cerebral blood flow and the reciprocal of the speckle decorrelation time. Previous data by several groups [10, 12] support use of this assumption

The linear response range of LSI depends on the image exposure time [10]. With conventional exposure times of 1 to 10 ms, this range can cover blood flow rates characteristic of arterioles and venules. To date, the limits of the linear response range have not been reported. For example, can the range be extended to rates characteristic of human cerebral vasculature?

Optical scattering diminishes the ability of LSI to enable visualization of subsurface microvasculature. In hypervascularized human skin, we instead visualize regions of tissue perfusion instead of individual blood vessels [13]. We encounter a similar outcome with LSI of subsurface tumor vasculature (unpublished data). Implementation of a method to enhance motion of intravascular particles would enhance LSI-based detection of low-flow vasculature.

The objective of this paper is to present two methods to extend the response range of LSI. We hypothesized that a decrease in image exposure time to sub-mm values, would enable extension of the linear response range to higher flow rates. Furthermore, based on previous studies using magnetic actuation of nanoparticles [14-18], we hypothesized that similar methodology would enhance the ability of LSI to visualize low-flow vasculature.

II. MATERIALS AND METHODS

A. LSI Instrument

The LSI instrument consists of a 633-nm HeNe laser and CCD camera. The laser was transmitted through a fiberoptic cable coupled to a computer-controlled attenuator, and finally focused to a spot size of 4 mm diameter. The resultant speckle pattern was imaged with a 12-bit monochrome CCD camera (Retiga EXi, QImaging, Surrey, British Columbia, Canada) equipped with a 90-mm Elicar macro lens. To maximize speckle contrast, the f/# of the lens was set to achieve a minimum speckle size equal to the width of approximately two camera pixels (individual pixel pitch = 6.5 μm) [19]. All image acquisition and data processing were done using custom LabVIEW software (Version 7.1, National Instruments, Austin, TX).

B. Flow Phantoms

1) Silicone Flow Phantom—To simulate superficial blood flow in biological tissue, a solid epoxy phantom was synthesized. Titanium dioxide particles suspended in the epoxy were used as scatterers. A glass capillary tube (1 mm inner diameter) was embedded at the surface of the phantom to mimic a blood vessel. With a syringe-based displacement pump (Pump 11 Plus, Harvard Apparatus, Holliston, MA), rabbit blood infused with heparin (anticoagulant) was pumped through the capillary tube. Software written in LabVIEW (Version 7.1, National Instruments, Austin, TX) was used to control the pump.

2) Capillary Tube—For the magnetomotive LSI experiments, a capillary tube (inner diameter of 500 μm) filled with nanoparticles (see next section) was used as the test substrate.

C. Iron Oxide Nanoparticles

Colloidal suspensions of superparamagnetic iron oxide (SPIO) nanoparticles are tissue-specific MRI contrast agents approved in 1996 by the United States Food and Drug Administration (FDA) for human use. Mean core diameter of these particles is 20 nm and total aggregation diameter is about 100 nm. SPIO nanoparticles consist of nonstoichiometric magnetite crystalline cores, iron, and a dextran T-10 coating that is used to prevent aggregation and provide stabilization in the liver. Feridex I.V. SPIO nanoparticles (Advanced Magnetics, Inc.) with a 5nm core diameter and dextran coating giving a nominal 100 nm diameter were used in all experiments. The prepared nanoparticle solution consisted of 50 mL 5% dextrose solution and 1 mL pure Feridex I.V. with a concentration of 0.67×10^{12} iron particles/μL (1.12 μg iron/μL) [20].

D. Magnet

A solenoid coil (manufacturer: Ledex, part number: 4EF) with a cone-shaped ferrite core at the center and driven by a current amplifier supplying up to 960 W, was placed underneath the sample during LSI. The combination of the core and solenoid, using high power operation, dramatically increased the magnetic field strength (B_{max}=1 T and field gradient of 220 T/m) at the tip of the core and also focused the magnetic force on the targeted samples.

The magnetic force applied to the capillary tube was varied by a sinusoidal current to induce SPIO nanoparticle movement.

E. Methods

1) General data collection protocol—After adjusting the pump settings, we activated the pump. After ~10 s, we manually initiated collection of a sequence of raw speckle images. Based on preliminary experiments, we determined empirically that 10 s was a sufficient period of time to achieve a steady flow rate.

2) High-flow rate experiments—Image exposure times of 10, 1, 0.1, and 0.01 ms were used. For reference, typical exposure times of 5 to 15 ms are reported in the peer-reviewed literature [1, 10, 21]. The range of average blood flow rate was dependent on the exposure time: 0-40 mm/s at T = 10 ms, 0-75 mm/s at T=1 ms, and 0-280 mm/s at T = 0.1 and 0.01 ms. For each exposure time, the flow rate was increased from zero flow conditions to the maximum value. For each pair of flow velocity and exposure time, a sequence of five raw speckle images was collected at 18 frames per s.

3) Magnetomotive LSI—For these experiments, we used a solution of SPIO nanoparticles as the medium, and we fixed the image exposure time at 10 ms. Prior to activation of the magnet, we collected a sequence of raw speckle images as described above. After manual activation of the magnetic field, we collected a second sequence of raw speckle images.

4) Data analysis—After data collection was complete, each image was converted to a speckle contrasθt image using a 7×7 sliding window operator, as described previously [22]. With the simplified speckle imaging equation presented independently by both Cheng and Duong [11] and Ramirez-San-Juan et al. [23], each speckle contrast image was converted to a speckle flow index (SFI) map:

$$SFI(i,j) = \frac{1}{\tau_c} = \frac{1}{TC(i,j)^2}$$

where (i,j) are the pixel coordinates in the image, τ_C is the speckle decorrelation time [s], T is the exposure time [s], and C(i,j) is the speckle contrast at pixel (i,j). Briers [24] proposed that τ_C is equivalent to the correlation time which is extracted from dynamic light scattering measurements. Dunn et al. [1] present empirical data which strongly suggest that SFI values are equivalent to the perfusion units associated with laser Doppler flowmetry.

For the high-flow-rate experiments, each set of five SFI images was averaged to compute a mean SFI image. From each mean SFI image, the SFI values within a 30 × 100 (0.2 mm × 0.65 mm) pixel region of interest from the center of the capillary tube were averaged. Hence, the effective frame rate was 3.6 frames per s (~280 ms temporal resolution).

III. RESULTS AND DISCUSSION

A. Characterization of High Blood Flow Rates

We analyzed LSI data collected from the flow phantom, with the independent variables being flow velocity and camera exposure time. With an exposure time of 10 ms, there was a linear relationship (R^2 = 0.98) between SFI values and flow velocity over 0 to 10 mm/s (Figure 1). At a flow velocity greater than 10 mm/s, the response was nonlinear and noise effects become very prominent. With an exposure time of 0.01 ms, the linear response range (R^2 = 0.99) extended to 280 mm/s. It is important to note that this upper bound was due to

hardware limitations of our flow phantom and not necessarily due to limits of the LSI instrument. However, for an exposure time of 0.01 ms, sensitivity to the lower velocities was diminished. Specifically, for an exposure time of 0.01 ms, our instrument was insensitive to flow rates less than 10 mm/s.

In humans, the diameter of pial arteries is 200 to 1200 μm [25] and the diameter of middle cerebral arteries is ~3000 μm [26]. For a group of 10 children, the flow velocity of the middle cerebral artery was measured as 690 mm/s [27]. Our *in vitro* data suggest that with use of a 0.01 ms exposure time, the LSI linear response range can extend out to flow speeds of at least 280 mm/s. Due to instrumentation limitations, we unfortunately were unable to evaluate the degree of linearity present between SFI values and flow speed, at faster speeds. Nevertheless, our data suggest the possibility of quantitative characterization of flow dynamics in the middle cerebral artery of pediatric patients and in human pial arteries. Such characterization may complement current methods which employ near-infrared imaging to study brain surface hemodynamics in children during neurosurgical procedures such as bypass surgery [28].

B. Magnetomotive LSI

With application of an AC magnetic field to a solution of stagnant SPIO particles, an apparent increase in SFI can be induced [Figure 2(A,B)]. With our specific configuration, we observed a ~3× increase in SFI values after the magnet is activated.

These results have broader implications for *in vivo* diagnostic and therapeutic applications. Oh et al. previously demonstrated that magnetic activation of monocrystalline iron oxide nanoparticles contained within macrophages, can enhance ultrasound [17] and OCT image contrast [18]. With judicious selection of magnetic field paramameters, it may be possible to enhance wide-field speckle contrast, and hence detectability, of tumors. Tumor blood flow typically is sluggish and thus is capable of inducing only a minor decrease at best in speckle contrast. With infusion of SPIO nanoparticles into the circulatory system and subsequent activation with an AC magnetic field, we expect that an appreciable decrease in speckle contrast would result. Use of surface markers, such as monoclonal antibodies, to enable molecular targeting of specific receptors (i.e., epidermal growth factor receptor [16], is expected to provide a mechanism for SPIO or similar nanoparticles to localize specifically within cancer cells and hence provide an additional source of specific speckle contrast reduction with magnetic activation.

Acknowledgments

B. Choi thanks Dr. Jeehyun Kim (Kyungpook National University, Republic of Korea) and Mr. Tyson Ringold (Purdue University) for assistance with data collection.

This work was supported in part by the Arnold and Mabel Beckman Foundation, A. Ward Ford Foundation, and the National Institutes of Health Laser Microbeam and Medical Program (LAMMP, a P41 Technology Research Resource).

REFERENCES

1. Dunn AK, Bolay T, Moskowitz MA, Boas DA. Dynamic imaging of cerebral blood flow using laser speckle. Journal of Cerebral Blood Flow and Metabolism. 2001; 21:195–201. [PubMed: 11295873]
2. Strong AJ, Bezzina EL, Anderson PBJ, Boutelle MG, Hopwood SE, Dunn AK. Evaluation of laser speckle flowmetry for imaging cortical perfusion in experimental stroke studies: quantitation of perfusion and detection of peri-infarct depolarisations. Journal of Cerebral Blood Flow and Metabolism. 2006; 26:645–653. [PubMed: 16251884]

3. Zhou C, Shimazu T, Durduran T, Luckl J, Kimberg DY, Yu GQ, Chen XH, Detre JA, Yodh AG, Greenberg JH. Acute functional recovery of cerebral blood flow after forebrain ischemia in rat. Journal of Cerebral Blood Flow and Metabolism. 2008; 28:1275–1284. [PubMed: 18382471]
4. Le TM, Paul JS, Al-Nashash H, Tan A, Luft AR, Sheu FS, Ong SH. New insights into image processing of cortical blood flow monitors using laser speckle imaging. Ieee Transactions on Medical Imaging. 2007; 26:833–842. [PubMed: 17679334]
5. Murari K, Li N, Rege A, Jia X, All A, Thakor N. Contrast-enhanced imaging of cerebral vasculature with laser speckle. Optics. 2007; 46:5340–5346.
6. Wang Z, Li PC, Luo WH, Chen SB, Luo QM. Peri-infarct temporal changes in intrinsic optical signal during spreading depression in focal ischemic rat cortex. Neuroscience Letters. 2007; 424:133–138. [PubMed: 17714868]
7. Royl G, Leithner C, Sellien H, Muller JP, Megow D, Offenhauser N, Steinbrink J, Kohl-Bareis M, Dirnagl U, Lindauer U. Functional imaging with laser speckle contrast analysis: Vascular compartment analysis and correlation with Laser Doppler Flowmetry and somatosensory evoked potentials. Brain Research. 2006; 1121:95–103. [PubMed: 17030028]
8. Choi B, Jia WC, Channual J, Kelly KM, Lotfi J. The importance of long-term monitoring to evaluate the microvascular response to light-based therapies. Journal of Investigative Dermatology. 2008; 128:485–488. [PubMed: 17657245]
9. Ayata C, Dunn AK, Gursoy-Ozdemir Y, Huang ZH, Boas DA, Moskowitz MA. Laser speckle flowmetry for the study of cerebrovascular physiology in normal and ischemic mouse cortex. Journal of Cerebral Blood Flow and Metabolism. 2004; 24:744–755. [PubMed: 15241182]
10. Choi B, Ramirez-San-Juan JC, Lotfi J, Nelson JS. Linear response range characterization and in vivo application of laser speckle imaging of blood flow dynamics. Journal of Biomedical Optics. 2006; 11:041129. [PubMed: 16965157]
11. Cheng HY, Duong TQ. Simplified laser-speckle-imaging analysis method and its application to retinal blood flow imaging. Optics Letters. 2007; 32:2188–2190. [PubMed: 17671579]
12. Parthasarathy AB, Tom WJ, Gopal A, Zhang XJ, Dunn AK. Robust flow measurement with multi-exposure speckle imaging. Optics Express. 2008; 16:1975–1989. [PubMed: 18542277]
13. Huang YC, Ringold TL, Nelson JS, Choi B. Noninvasive blood flow imaging for real-time feedback during laser therapy of port wine stain birthmarks. Lasers in Surgery and Medicine. 2008; 40:167–173. [PubMed: 18366081]
14. Kim J, Oh J, Milner TE, Nelson JS. Imaging nanoparticle flow using magneto-motive optical Doppler tomography,"x Nanotechnology. 2007; 18:035504.
15. Oldenburg AL, Gunther JR, Boppart SA. Imaging magnetically labeled cells with magnetomotive optical coherence tomography. Optics Letters. 2005; 30:747–749. [PubMed: 15832926]
16. Aaron JS, Oh J, Larson TA, Kumar S, Milner TE, Sokolov KV. Increased optical contrast in imaging of epidermal growth factor receptor using magnetically actuated hybrid gold/iron oxide nanoparticles. Optics Express. 2006; 14:12930–12943. [PubMed: 19532186]
17. Oh J, Feldman MD, Kim J, Condit C, Emelianov S, Milner TE. Detection of magnetic nanoparticles in tissue using magnetomotive ultrasound. Nanotechnology. 2006; 17:4183–4190. [PubMed: 21727557]
18. Oh J, Feldman MD, Kim J, Kang HW, Sanghi P, Milner TE. Magneto-motive detection of tissue-based macrophages by differential phase optical coherence tomography. Lasers in Surgery and Medicine. 2007; 39:266–272. [PubMed: 17295337]
19. Kirkpatrick SJ, Duncan DD, Wells-Gray EM. Detrimental effects of speckle-pixel size matching in laser speckle contrast imaging. Optics Letters. 2008; 33:2886–2888. [PubMed: 19079481]
20. Artemov D. Molecular magnetic resonance imaging with targeted contrast agents. Journal of Cellular Biochemistry. 2003; 90:518–524. [PubMed: 14523986]
21. Yuan S, Devor A, Boas DA, Dunn AK. Determination of optimal exposure time for imaging of blood flow changes with laser speckle contrast imaging. Applied Optics. 2005; 44:1823–1830. [PubMed: 15813518]
22. Briers JD, Richards G, He XW. Capillary blood flow monitoring using laser speckle contrast analysis (LASCA). Journal of Biomedical Optics. 1999; 4:164–175. [PubMed: 23015182]

23. Ramirez-San-Juan JC, Ramos-Garcia R, Guizar-Iturbide I, Martinez-Niconoff G, Choi B. Impact of velocity distribution assumption on simplified laser speckle imaging equation. Optics Express. 2008; 16:3197–3203. [PubMed: 18542407]

24. Briers JD. Laser Doppler and time-varying speckle: A reconciliation. Journal of the Optical Society of America a-Optics Image Science and Vision. 1996; 13:345–350.

25. ThorinTrescases N, Bartolotta T, Hyman N, Penar PL, Walter CL, Bevan RD, Bevan JA. Diameter dependence of myogenic tone of human pial arteries - Possible relation to distensibility. Stroke. 1997; 28:2486–2492. [PubMed: 9412638]

26. Serrador JM, Picot PA, Rutt BK, Shoemaker JK, Bondar RL. MRI measures of middle cerebral artery diameter in conscious humans during simulated orthostasis. Stroke. 2000; 31:1672–1678. [PubMed: 10884472]

27. Soriano SG, McManus ML, Sullivan LJ, Rockoff MA, Black PML, Burrows FA. Cerebral blood flow velocity after mannitol infusion in children. Canadian Journal of Anaesthesia-Journal Canadien D Anesthesie. 1996; 43:461–466. [PubMed: 8723852]

28. Nakagawa A, Fujimura M, Arafune T, Sakuma I, Tominaga T. Intraoperative infrared brain surface blood flow monitoring during superficial temporal artery-middle cerebral artery anastomosis in patients with childhood moyamoya disease. Childs Nervous System. 2008; 24:1299–1305.

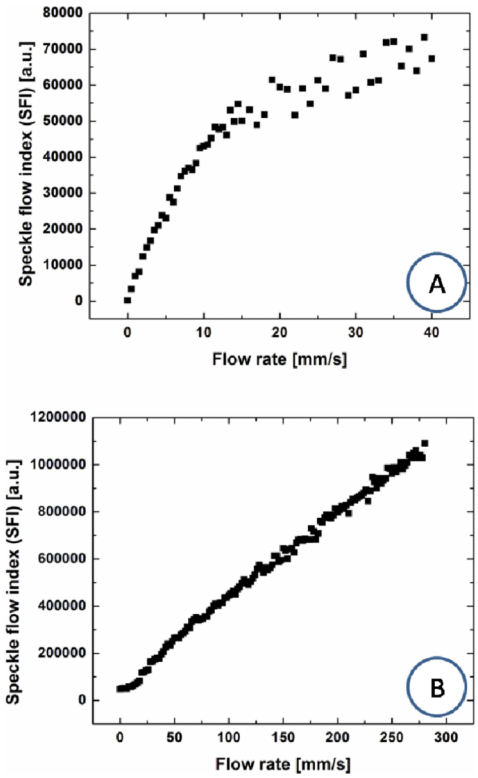

Fig. 1.

Camera exposure time affects the linear response range of LSI. Raw speckle images collected from an *in vitro* blood flow phantom were converted to speckle contrast (not shown here) and ultimately to SFI images. Mean SFI values were computed from a ROI within the lateral boundaries of the flow tube. With typical exposure times of (A) 10 1 ms, a linear response range of 0 to 10 mm/s was achieved. With a further reduction in exposure time to (B) 0.01 ms, the linear response range was extended to 280 mm/s. Note that this 280 mm/s upper limit was imposed by our experimental setup.

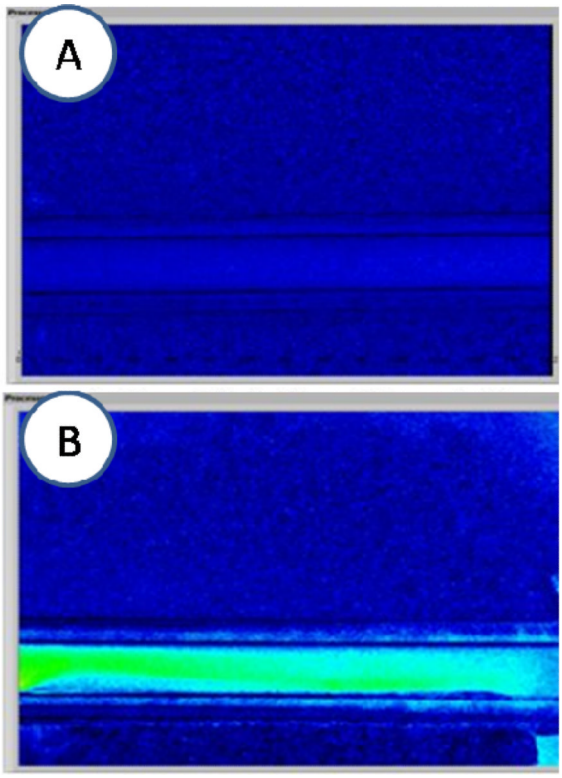

Fig. 2.
Representative data from experiments involving magnetic actuation of SPIO nanoparticles. (A) Speckle flow index (SFI) image in absence of magnetic field. (B) Speckle flow index image after activation of AC magnetic field, with a clear increase in SFI values.